

The proliferation of malignant melanoma cells could be inhibited by ranibizumab via antagonizing VEGF through VEGFR1

Jiao Li,¹ Yan Cui,² Qin Wang,³ Dadong Guo,² Xuemei Pan,¹ Xingrong Wang,¹ Hongsheng Bi,¹ Wei Chen,¹ Zhengfeng Liu,⁴ Shengya Zhao¹

(The first two authors contributed equally to this work.)

¹Affiliated Eye Hospital of Shandong University of Traditional Chinese Medicine, Jinan, Shandong, Peoples' Republic of China;

²Eye Institute of Shandong University of TCM, Jinan, Shandong, Peoples' Republic of China; ³People's Hospital of Rizhao, Rizhao, Shandong, Peoples' Republic of China; ⁴Shandong University of Traditional Chinese Medicine, Jinan, Shandong, Peoples' Republic of China

Purpose: Angiogenesis is an important mediator in tumor progression. Vascular endothelial growth factor (VEGF) is one of the major cytokines that can influence angiogenesis. However, the potential mechanism of tumor growth inhibition through anti-VEGF agents is still unclear. This study was performed to examine whether ranibizumab could inhibit malignant melanoma growth in vitro and to determine the safety of ranibizumab on human adult retinal pigment epithelium cell line (ARPE-19 cells).

Methods: Malignant melanoma cells obtained from a clinic were cultured in vitro. VEGF concentrations secreted by malignant melanoma cells and the ARPE-19 cells were examined by enzyme-linked immunosorbent assay (ELISA). The two kinds of cells were both treated with VEGF and its antagonist, ranibizumab. The dynamic changes of the two types of cells were monitored by real-time cell electronic sensing (RT-CES) assay. The effect of ranibizumab on both types of cells was verified by 3-(4,5-dimethylthiazol-2-yl)-2,5-diphenyl (MTT) assay. The expression of VEGF receptor 1 (VEGFR1) RNA in uveal melanoma was further investigated through the PCR technique.

Results: The levels of VEGF secreted by malignant melanoma cells were much higher than those of ARPE-19 cells, and were markedly decreased in the action of 0.1 mg/ml ranibizumab. However, there was no obvious reduction of VEGF in the presence of ranibizumab for ARPE-19 ($p > 0.05$). Meanwhile, RT-CES showed that the viability of malignant melanoma cells increased greatly in the presence of VEGF. When VEGF was 20 ng/ml, viability of the malignant melanoma cells increased by 40% compared with the negative control. There was no evident effect on proliferation of ARPE-19 ($p > 0.05$). Furthermore, the growth of malignant melanoma cells was obviously inhibited after ranibizumab intervention. When ranibizumab was administered at 0.25 mg/ml, the survival rate of the malignant melanoma cells decreased to 57.5%. Nevertheless, low-dose exposure to ranibizumab had only a slight effect on the growth of ARPE-19, and PCR result demonstrated that VEGFR1 plays a role in this tumor tissue rather than VEGFR2.

Conclusions: Ranibizumab can selectively inhibit malignant melanoma cell proliferation by decreasing the expression of VEGF; the possible mechanism of the inhibitory effect may involve VEGFR1 antagonism.

Vascular endothelial growth factor (VEGF) was first described as a molecule that could increase the permeability of blood vessels. Additionally, VEGF promotes the proliferation of new blood vessels, and is essential for normal embryonic development and wound healing. There is an obvious correlation between intensity of VEGF and tumor prognosis [1]. VEGF encompasses a family of proteins that include placenta growth factor (PlGF), VEGF-A, VEGF-B, VEGF-C, VEGF-D, and VEGF-E. The VEGF receptor (VEGFR) family in mammals contains three members, namely VEGFR1,

VEGFR2, and VEGFR3. These factors directly participate in the genesis of blood capillaries and lymphatic vessels [2-7].

Three anti-VEGF agents—pegaptanib, bevacizumab, and ranibizumab [8]—have been used for the treatment of patients with neovascularization pathology. Ranibizumab (Lucentis®, Genentech, Inc., South San Francisco, CA) is a recombinant humanized immunoglobulin designed for intraocular use which can bind to and inhibits the biological activity of human VEGF-A [9]. It has been shown to be safe and effective when given intravitreally to patients with neovascular wet age-related macular degeneration (AMD). In addition, ranibizumab has recently been approved for diabetic macular edema (DME) therapy [10]. Bevacizumab (Avastin®, Genentech, Inc.) a full-length, humanized, monoclonal antibody against all types of VEGF, is the most commonly used drug in the United States for the treatment of neovascular

Correspondence to: Xingrong Wang, Affiliated Eye Hospital of Shandong University of TCM, Jinan, Shandong, Peoples' Republic of China. 48 Jinan Yingxiongshan Road, Shandong, Peoples' Republic of China, 250002. Phone: +86 18764040527; FAX: +86 0531-82861167; email: wangxr0928@163.com.

AMD. It is currently approved for the treatment of metastatic colorectal cancer [11]. A case series to date by Finger and Chin on 21 patients with iodine-125 brachytherapy-induced radiation maculopathy found that administration of 1.25 mg/0.05 ml of bevacizumab led to decreased macular edema, improved or maintained visual acuity, and reduced hemorrhage and retinal edema [12]. One report focused on a man whose ocular history included brachytherapy with ruthenium plaque for choroidal melanoma 15 months previously; it was confirmed that intravitreal bevacizumab could ameliorate the decline in visual acuity caused by radiation maculopathy [13].

Tumor growth is angiogenesis dependent, and therapy targeting tumor vasculature is an attractive alternative or adjunct to conventional therapy. VEGF is important in several malignant and nonmalignant pathologies. Previously, it was shown that selective inhibition of VEGF binding to VEGFR2 with a fully human monoclonal antibody (r84) is sufficient for effective control of tumor growth in a preclinical model of breast cancer [14]. One report demonstrated the effectiveness of anti-VEGF therapy as a modulator of immune cell infiltration, as well as intratumoral and serum cytokine levels, in multiple preclinical models of breast cancer [15]. In metastatic colorectal cancer, an objective response rate of 3.3% was observed among chemotherapy-pretreated patients receiving monotherapy with bevacizumab [16]. Trials of bevacizumab with chemotherapy as the first-line treatment for metastatic non-small-cell lung cancer have yielded the results of improving patient outcomes [17,18].

We were interested in exploring whether ranibizumab, the anti-VEGF agent, would result in novel efficacy against ocular tumor. In addition, we intended to evaluate the safety of ranibizumab. In the present study, the effects of VEGF on malignant melanoma cells of the ciliary body and on the human adult RPE cell line (ARPE-19) were investigated to determine whether the growth of two kinds of cells is VEGF dependent, and the inhibitory mechanism of ranibizumab on the growth of tumor cells and ocular safety was also explored.

METHODS

The study was performed in the Affiliated Eye Hospital of Shandong University of Traditional Chinese Medicine. All measurements adhered to the tenets of the Helsinki agreement.

Primary culture of ocular malignant melanoma and culture of the ARPE-19 cell line: Malignant melanoma of the ciliary body was derived from a female inpatient in our hospital. A part of the tumor tissue was fixed by 10% formaldehyde solution. Paraffin sections from the tissue were examined

with hematoxylin and eosin (H&E) staining. Immunohistochemical staining of HMB-45, S-100 protein, and Melan-A (Golden Bridge Biotechnology Company Ltd., Peking, China) were performed for identification of melanoma. The other part of the tumor tissue was cultured in RPMI 1640 medium (HyClone, Tianjin, China) with 10% fetal bovine serum (FBS; HyClone) after digestion with 0.05% trypsin. The following experiments were carried out with three to six cell passages.

The human RPE cell line (ARPE-19) was obtained from the American Type Cell Culture (ATCC, Manassas, VA); it matched for the ATCC human cell line CRL-2302. The ARPE-19 cell was verified by the ATCC Cell Line Authentication Service (Promega, Madison, WI) using short tandem repeat analysis and an amelogenin gender-determining locus, as shown in Table 1. The cells were used between passages 3 and 6. Cells were maintained in the same medium as melanoma cells, that is, RPMI 1640 with 10% FBS. All cells were cultured at 37 °C in a 5% CO₂ incubator with a humidified environment.

Melanoma cell identification by immunocytochemistry: Malignant melanoma cells of the ciliary body were cultured primarily in the laboratory and cells between the third and the sixth generation were used in the experiments. When they had reached 80–90% confluence, cells were digested with 0.05% trypsin. After washing twice with PBS, the cell pellet was smeared onto three pieces of slides for immunocytochemistry staining with HMB-45, S-100 protein, and Melan-A, respectively.

VEGF secretion detected by ELISA: To determine the VEGF level secreted by malignant melanoma cells and ARPE-19, 200 µl supernatant was collected from the media after 24 h culture in the absence and presence of 0.1, 0.25, 0.5, and 1 mg/ml of ranibizumab. The concentration was measured using a VEGF ELISA kit (R&D, Minneapolis, MN) following the suggested protocol. The optical densities were determined within 30 min and recorded with a microplate reader (BioTek, EXL800, Winooski, VT) at 450 nm.

Real-time cell electronic sensing assay: First, 1×10⁴ malignant melanoma cells or ARPE-19 were seeded into each well of a 16-well plate containing 100 µl of culture medium and incubated for 20 h in a 5% CO₂ incubator. After removing the medium, the VEGF solution (Pepro Tech Inc., Suzhou, China) was diluted with fresh RPMI 1640 medium and then added into each well with final concentrations of VEGF 0, 1, 5, 10, and 20 ng/ml. Each concentration was set in triplicate.

Second, the medium was removed after 20 h of incubation for the two kinds of cells. The final concentrations of ranibizumab in malignant melanoma cells and ARPE-19 were

TABLE 1. STR GENOTYPE AND AMELOGENIN GENDER-DETERMINING LOCUS OF ARPE-19 CELL USED.

Loci	Test results for submitted Sample		ATCC reference database profile	
	Query profile: ARPE-19(UCLA-19)		Database profile: ARPE-19	
D3S1358	14	15		
TH01	6	9.3	6	9.3
D21S11	28	29		
D18S51	12	16		
Penta_E	7	11		
D5S818	13		13	
D13S317	11	12	11	12
D7S820	9	11	9	11
D16S539	9	11	9	11
CSF1PO	11		11	
Penta_D	11	13		
Amelogenin	X	Y	X	Y
vWA	16	19	16	19
D8S1179	13			
TPOX	9	11	9	11
FGA	23			
D19S433	12	13		
D2S1338	19			
Number of shared alleles between query sample and database profile:			16	
Total number of alleles in the database profile:			16	
Percent match between the submitted sample and the database profile:			100	

0, 0.1, 0.25, 0.5, and 1 mg/ml, respectively. Each concentration was set in triplicate.

Analyses for both experiments were conducted using an RT-CES analyzer (ACEA Biosciences Inc., Hangzhou, China) for at least 80 h and the cell culture medium volume used for detection was 200 μ l. The electrical impedance, displayed as a normalized cell index (NCI), was monitored and the dynamic changes induced by the interaction between cells and VEGF or ranibizumab was recorded.

RT-CES assay can provide dynamic information to identify the interaction between target cells and reagents. The RT-CES system monitors cellular events in real time by measuring the electrical impedance between microelectrodes integrated into the bottom of custom-made tissue culture plates (E-Plates). Since cells have a very high electrical resistance, the more cells are attached to the bottom of the E-Plates, the higher the electrical impedance will be. Thus, the electrical impedance, displayed as NCI, can be used to monitor cell viability, number, and adhesion in a large number of cell culture wells simultaneously, at any given frequency, and over any desired period of time without taking the plates

out of the incubator. The RT-CES assay has been proven to be a valuable and reliable approach to real-time monitoring of dynamic changes induced by cell-chemical interaction [19-22].

MTT assay: Based on the observations above, the potential effect of ranibizumab on melanoma cells and ARPE-19 cells was further investigated via MTT assay. First, 1×10^4 cells were seeded into each well containing 200 μ l cell culture medium in 96-well plates and incubated for 24 h in a 95% air and 5% CO₂ incubator. The ranibizumab solution was diluted with fresh RPMI 1640 medium and then added to the cultivated wells, where the final concentrations of ranibizumab in both cells' wells (in triplicate) were 0, 0.1, 0.25, 0.5, and 1 mg/ml, respectively. Wells without ranibizumab were used as the control experiments. After incubation for 24 h, 20 μ l of 5 mg/ml of MTT was added to each well, followed by further incubation for 4 h. The survival rate (%) was expressed as follows: survival rate (%) = $\frac{[A] \text{ ranibizumab}}{[A] \text{ control}} \times 100$, where A is the absorbance value of the relative sample at 490 nm. Every experiment was repeated at least three times.

Extraction of total RNA from formalin-fixed, paraffin-embedded tissue: Total RNA from the tumor was extracted from formalin-fixed, paraffin-embedded tissue using a modification of the method described by Rupp and Locker [23]. Briefly, RNA was extracted from ten 8 μ m sections, and further paraffin was removed by extracting twice with 1.5 ml of xylene for 10 min followed by rehydration through subsequent washes with 100, 90, and 70% ethanol diluted in RNase-free water; then the tissue was collected by centrifugation at 16,000 \times g for 5 min. After the final step with 70% ethanol rinse, the pellet was dried, resuspended in 200 ml of RNA lysis buffer containing 10 mmol/l Tris (pH 8.0), 0.1 mmol/l EDTA (pH 8.0), 2% sodium dodecyl sulfate (pH 7.3), and 500 mg/ml proteinase K (Sigma, Deisenhofen, Germany), and incubated at 60 °C for 16 h until the tissue was completely solubilized. The precipitate was removed and resuspended in 1 ml Trizol reagent (Aidlab Biotechnologies Co., Ltd., Peking, China) and incubated at 4 °C for 30 min. RNA was purified by phenol and chloroform extractions followed by precipitation with an equal volume of isopropanol for 30 min. The RNA pellet was washed once in 75% ethanol, dried, and resuspended in 20 μ l of RNase-free water; it was then quantified by a micro-spectrophotometer (K5600, Beijing Kaiya Technology Development Co., Ltd. Peking, China).

PCR determination: The total RNA was reverse transcribed using Moloney murine leukemia virus (M-MLV) reverse transcriptase (Aidlab Biotechnologies Co., Ltd.). PCR was performed on a TP600 reverse-transcription PCR (RT-PCR) system (Takara, Japan), according to the manufacturer's instructions. The primer sequences for human VEGF receptor 1 (VEGFR1) were 5'-TTT AAA AGG CAC CCA GCA CAT-3' (forward) and 5'-TTA CTC ACC ATT TCA GGC AAA GAC-3' (reverse); primer sequences for human VEGFR2 were 5'-GGC CCA ATA ATC AGA GTG GCA-3' (forward) and 5'-TGT CAT TTC CGA TCA CTT TTG GA-3' (reverse). The amplification conditions were as follows: 95 °C for 30 s and 40 cycles of 95 °C for 5 s and 57 °C for 34 s. PCR products were analyzed using agarose gel electrophoresis.

Statistical analysis: Data were expressed as the mean \pm SD (standard deviation) from at least three independent experiments. One-way analysis of variance (ANOVA) was used for significance testing, and $p < 0.05$ was considered statistically significant.

RESULTS

Histopathological observation of malignant melanoma of the ciliary body: The tumor was composed of fusiform and epithelioid malignant melanoma cells. The cytoplasm was abundant with melanin granules. The nuclei were big

with prominent nucleoli (Figure 1A). Additionally, paraffin sections were depigmented by KMnO_4 (potassium permanganate) before H&E staining (Figure 1B), and the tumor showed histopathological features of infiltrative growth. Immunohistochemical staining indicated that the tumor tissue expressed HMB-45 and S-100 positively (Figure 1C,E). Melan-A was weakly positive (Figure 1D). The positive expression was displayed as brown yellow located in cytoplasm. Melanin granules appeared dark green after cytoplasm was counterstained with Giemsa [24].

Malignant melanoma cell culture and immunocytochemical staining: The malignant melanoma cells were cultured at 37 °C in a 5% CO_2 humidified incubator. The cells appeared to have attached characteristics with a spindle shape, and were rich in melanin granules. During the course of culturing, the cells depigmented gradually (Figure 2A). Passaging to the fifth generation, the melanin granules disappeared completely (Figure 2B). Immunocytochemical staining indicated positive expression of S-100 (Figure 2E) and weak positive expression of HMB-45 and Melan-A (Figure 2C, D). The positive expression is located in the cytoplasm with a brown-yellow color. PBS solution was used as the primary antibody in the negative control for immunohistochemical staining and immunocytochemical staining.

Malignant melanoma cells secrete more VEGF than ARPE-19 cells: We determined the levels of VEGF of the supernatant from the two kinds of cells with or without ranibizumab by ELISA. Untreated malignant melanoma cells expressed 1533.4 ± 7 pg/ml VEGF (Figure 3); the mean levels of VEGF of malignant melanoma cells after 24 h exposure to 0.1, 0.25, 0.50, and 1 mg/ml of ranibizumab were 822.55 ± 9.3 pg/ml, 875.02 ± 7.8 pg/ml, 836.13 ± 6.3 pg/ml, and 844.8 ± 6 pg/ml, respectively. ARPE-19 without ranibizumab expressed 908.75 ± 9.1 pg/ml VEGF, and the mean levels of VEGF of ARPE-19 cells after 24 h exposure to 0.1, 0.25, 0.50, and 1 mg/ml ranibizumab were 891.1 ± 7.3 pg/ml, 828 ± 5 pg/ml, 767 ± 4.5 pg/ml, and 870 ± 6.2 pg/ml, respectively.

RT-CES dynamic study for the effect of VEGF and ranibizumab on malignant melanoma cells and ARPE-19 showed that tumor cells are more inclined to be inhibited by ranibizumab: Malignant melanoma and ARPE-19 cells were treated with 1, 5, 10, and 20 ng/ml of VEGF. After adding VEGF to the malignant melanoma cells (Figure 4A), NCI was higher compared with the cells without VEGF. What is more, NCI became higher kinetically following the culture time ($p < 0.05$). VEGF had a significant influence on the viability of malignant melanoma cells. When VEGF was 5, 10, and 20 ng/ml, the malignant melanoma cells' viability increased by 18%, 20%, and 40%, respectively, compared with the

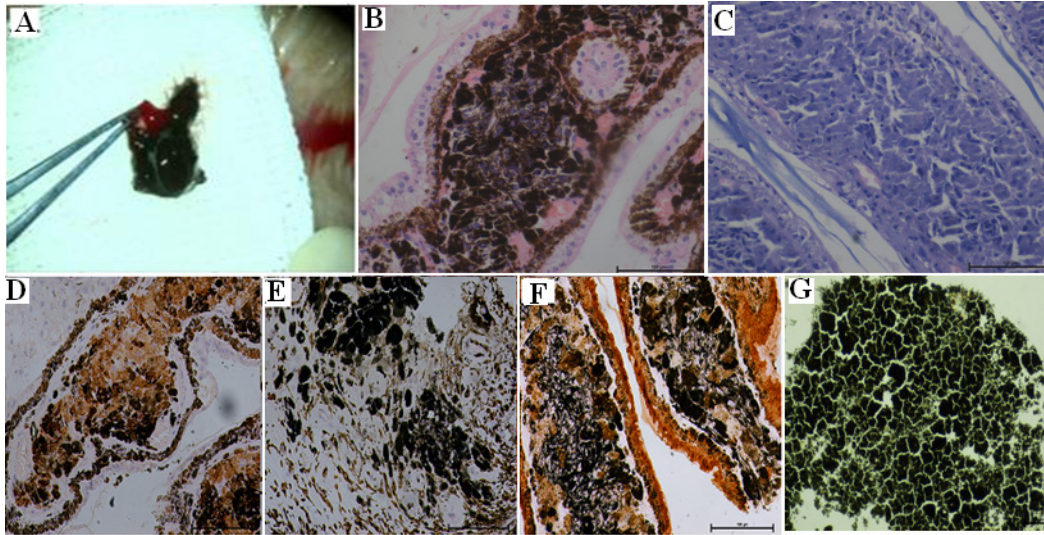


Figure 1. An overview, hematoxylin and eosin (H&E) staining, and immunohistochemical staining of malignant melanoma. **A:** An overview of the tumor. **B:** H&E staining of the tissue of malignant melanoma. **C:** H&E staining depigmented by KMnO_4 (potassium permanganate) of malignant melanoma. The tissue was constituted by fusiform and epithelioid malignant melanoma cells. Cytoplasm was abundant with melanin granules. Nuclei was big with prominent nucleoli. **D:** Expression of HMB-45 in immunohistochemical staining of malignant melanoma was positive. **E:** Expression of Melan-A was weakly positive; **F:** Expression of S-100 protein was positive. **G:** Negative control. DAB was used as chromogen. (magnification: 200 \times).

untreated cells (Figure 4B). This increase effected by VEGF was dose dependent.

There was no evident effect of VEGF on cell proliferation of ARPE-19 cells. As shown in Figure 4C,D, we observed that NCI decreased slightly compared with the untreated cells when VEGF was 1, 5, 10, or 20 ng/ml.

The observations demonstrated that when ranibizumab was added to the malignant melanoma cell system, the NCI was lower compared to that of cells without ranibizumab treatment (Figure 5A). Moreover, the NCI decreased following the culture time ($p < 0.05$). The results indicate that ranibizumab has an inhibitory effect on the growth of malignant melanoma cells. Furthermore, this inhibitory effect induced by ranibizumab was also dose dependent. When ranibizumab

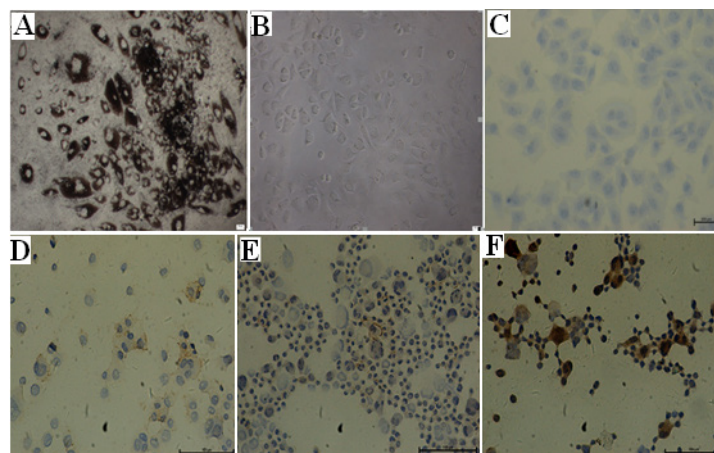


Figure 2. Cell culture and immunohistochemical staining of malignant melanoma cells. The cells appeared with attached characteristics; they were spindle-shaped and rich in melanin granules. **A:** Depigmented cells during the course of culturing. **B:** Cells passaging to the fifth generation. The melanin granules disappeared completely. **C:** Illustrates the negative control for immunocytochemical staining. **D:** Weak positive expression of HMB-45. **E:** Weak positive expression of Melan-A. **F:** Positive expression of S-100 (magnification: 200 \times).

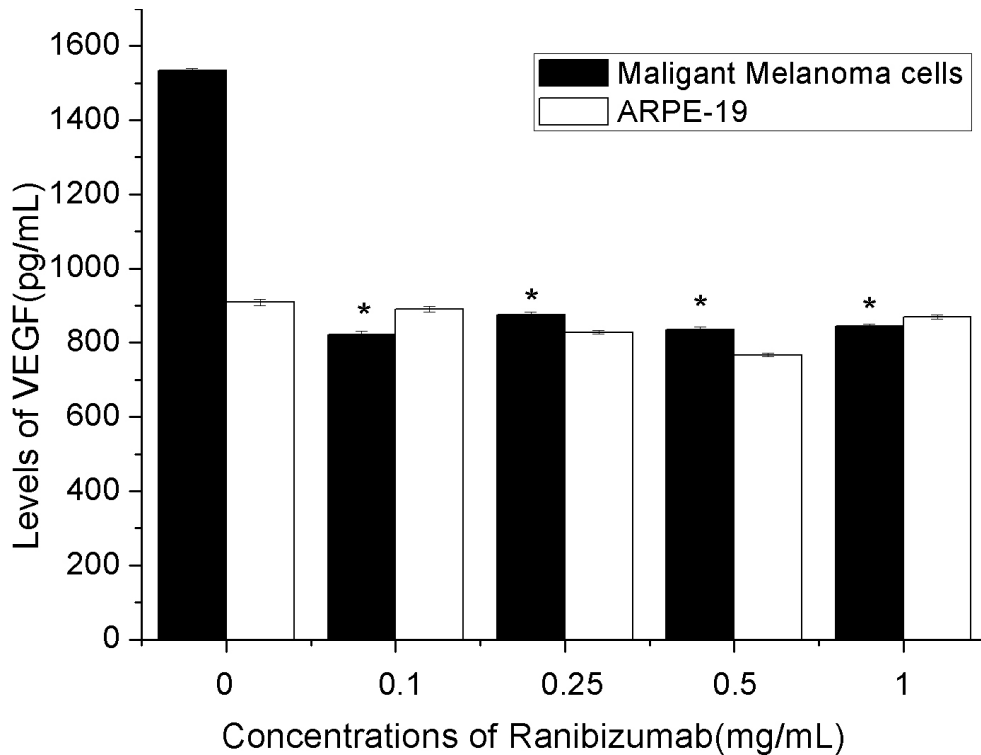


Figure 3. Levels of vascular endothelial growth factor (VEGF) of malignant melanoma cells and ARPE-19 cells in the absence and presence of ranibizumab. Cell supernatants were assayed for enzyme-linked immunosorbent assay (ELISA) as described in the methods section. * $p < 0.05$ compared to untreated cells. Data represents three independent experiment and all data points plotted as mean values \pm SD (* $p < 0.05$).

was 0.1 mg/ml, 0.25 mg/ml, and 0.5 mg/ml, the survival rates of malignant melanoma cells decreased to 12%, 57.5%, and 72% compared with the untreated cells (Figure 5B).

When ranibizumab was only 0.1 mg/ml, the electrode impedance decreased slightly compared with ARPE-19 without ranibizumab ($p > 0.05$). There was a decrease when ranibizumab increased to 0.25 mg/ml, and no evident difference in ARPE-19 proliferation treated with 0.5 mg/ml and 1 mg/ml ranibizumab; the survival rates of ARPE-19 were 55.6% and 42.8%, respectively (Figure 5C,D). The results indicate that a high dose of ranibizumab has an inhibitory effects on the growth of ARPE-19.

MTT assay for effects of ranibizumab on uveal melanoma and ARPE-19 cells: As shown in Figure 6, it was observed that the effect of ranibizumab on the two kinds of cells occurred in a dose-dependent manner, which was similar with the results for RT-CES. When ranibizumab was 0.1 mg/ml, 0.25 mg/ml, 0.5 mg/ml, and 1 mg/ml, the survival rates of malignant melanoma cells were 98.1%, 91.05%, 88.55%, and 79.2%, respectively, and the survival rates of ARPE-19 were 98.96%, 96.1%, 89.6%, and 88.03%, respectively. When ranibizumab was 0.1 mg/ml and 0.25 mg/ml, the surviving rate decreased slightly comparing with ARPE-19 without ranibizumab ($p = 0.77$, $p = 0.26$, respectively). There were remarkable decreases when ranibizumab increased to

0.25 mg/ml, 0.5 mg/ml, and 1 mg/ml for malignant melanoma cells ($p = 0.006$, $p = 0.001$, $p = 0.00$, respectively).

VEGFR1 expression in human malignant melanoma of the ciliary body: We examined the mRNA expression of VEGFR1 and VEGFR2 in malignant melanoma of the ciliary body by PCR. The results showed that the transcripts of VEGFR1 are present in this tumor tissue; on the other hand, VEGFR2 is not expressed (Figure 7). These results suggested that VEGFR1, but not VEGFR2, is likely to be involved in the inhibition of ranibizumab regarding malignant melanoma cells.

DISCUSSION

VEGF was originally identified as an endothelial cell-specific growth factor that can stimulate angiogenesis and enhance vascular permeability. VEGF-A is the most well-studied member of the VEGF family and is a key target for antiangiogenic therapy [25]. VEGFR1 regulates endothelial cell function indirectly through macrophage recruitment [26], followed by deposition of angiogenic growth factors by these cells. In monocytes, VEGFR1-specific ligands VEGF-B and PlGF both induce signaling pathways known to operate downstream of most tyrosine kinase receptors, such as extracellular signal-regulated kinase (ERK)/mitogen-activated protein kinase (MAPK), phosphatidylinositol-3-kinase

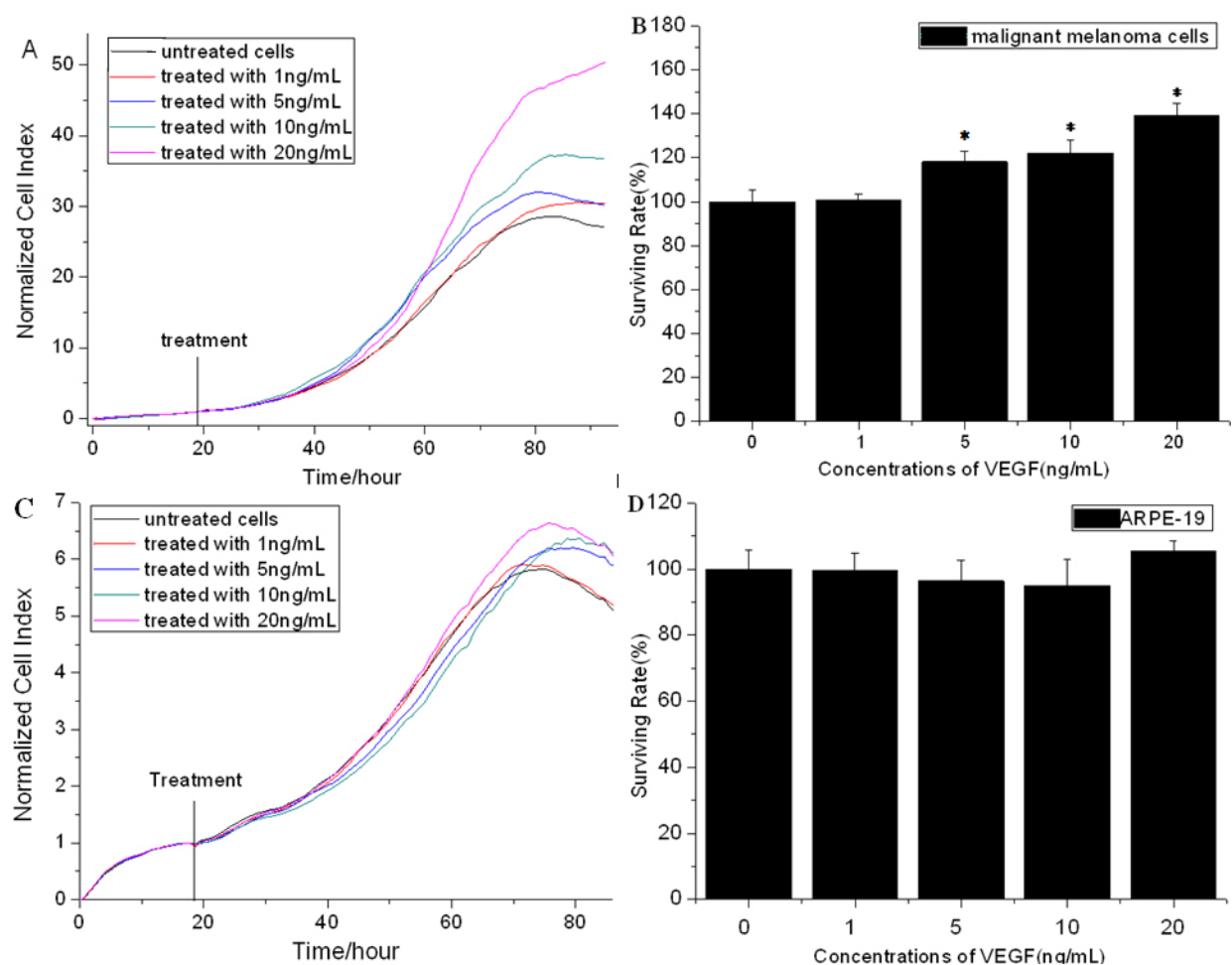


Figure 4. Dynamic response of malignant melanoma and ARPE-19 cell exposure to vascular endothelial growth factor (VEGF). **A** and **B** represent the dynamic response of malignant melanoma cells with different concentrations of VEGF, as follows: untreated malignant melanoma cells (control, 0 ng/ml); 1 ng/ml VEGF; 5 ng/ml VEGF; 10 ng/ml VEGF; and 20 ng/ml VEGF. **B**: Comparison of increases in cell activity in the presence of VEGF after malignant melanoma cells were incubated in the cell system for about 72 h. * $p < 0.05$ compared to untreated cells. **C** and **D** show the dynamic response of ARPE-19 with different concentrations of VEGF, as follows: untreated cells (control); 1 ng/ml VEGF; 5 ng/ml VEGF; 10 ng/ml VEGF; and 20 ng/ml VEGF. **D**: Comparison of increases in cell activity in the presence of VEGF after ARPE-19 were incubated in the cell system for about 72 h. * $p < 0.05$ compared to untreated cells. Data represents three independent experiment and all data points plotted as mean values \pm SD (* $p < 0.05$).

(PI3K)/protein kinase B (PKB/AKT), and the stress kinase p38MAPK [27], in which VEGFR1-mediated signaling pathways are essential for VEGFR1 biology in vivo. PIGF is also dispensable for embryonic and adult physiological angiogenesis [28], but promotes pathological angiogenesis in several diseases. Moreover, PIGF binds to neuropilin-1 (NRP-1). VEGFR1 is expressed by a broad range of cell types, including human tumor cells [29].

It now appears that VEGF also has autocrine functions acting as a survival factor for tumor cells, protecting them from stresses such as hypoxia, chemotherapy, and radiotherapy [30]. In cancer, tumor angiogenesis contributes to tumor growth and metastasis. An important step in

antiangiogenic cancer therapy was taken when the anti-VEGF blocking antibody bevacizumab showed remarkable results in the treatment of metastatic colorectal cancer, and it has been approved by the *Food and Drug Administration* (FDA) for treatment of metastatic colorectal cancer [31,32]. Ranibizumab is an affinity-matured antigen-binding fragment (Fab) derived from bevacizumab, and thus has a higher affinity for VEGF-A [33]. Ranibizumab was developed specifically for intravitreal administration to treat vascular eye diseases. Intravitreal injection of 0.5 mg of ranibizumab is recommended for patients with subfoveal choroidal neovascularization (CNV). However, the effect of ranibizumab on tumors has not been clearly identified.

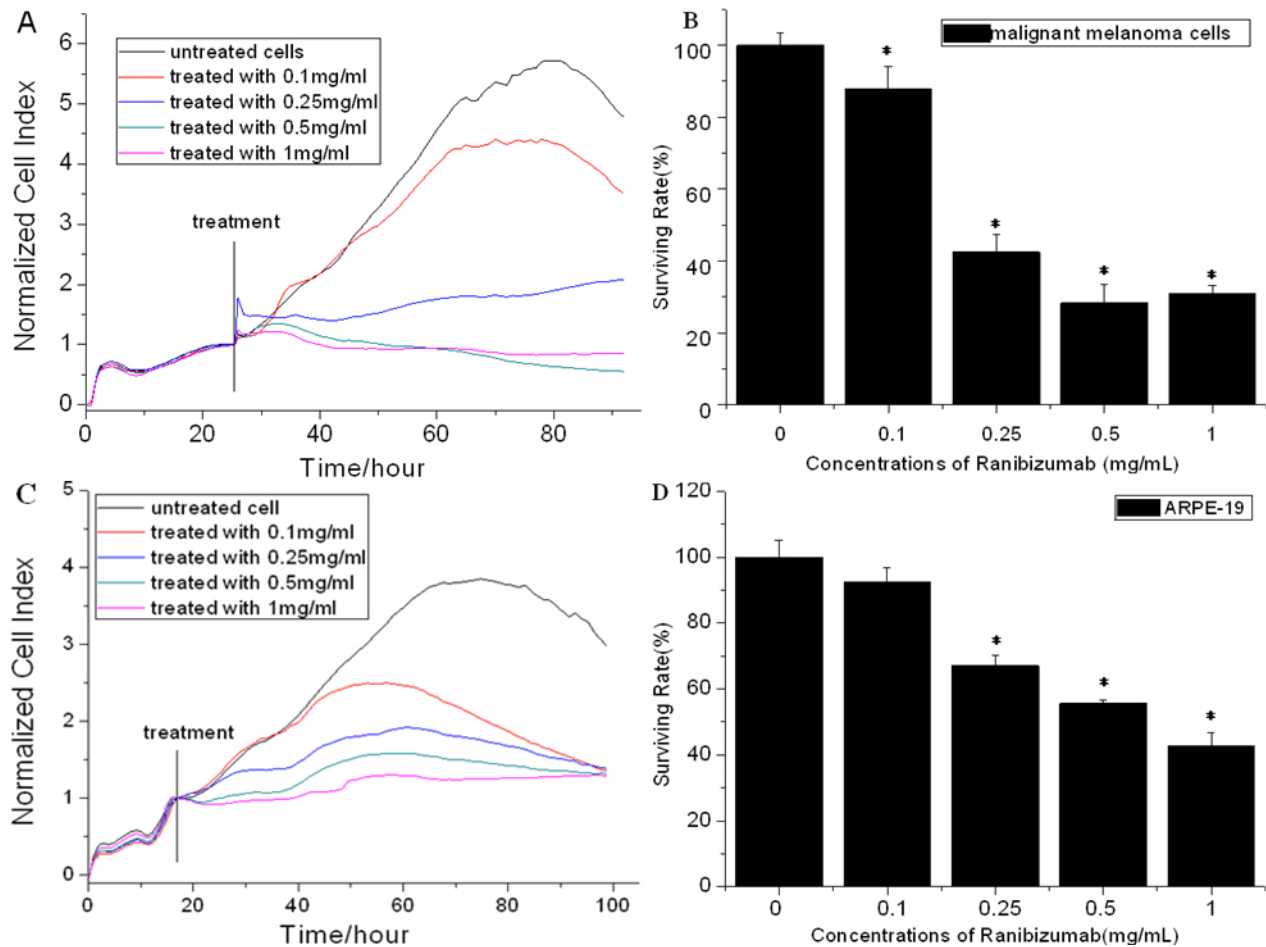


Figure 5. Dynamic response of malignant melanoma and ARPE-19 cell exposure to ranibizumab. **A** and **B** represent the dynamic response of malignant melanoma cells with different concentrations of ranibizumab, as follows: untreated cells (control); 0.1 mg/ml; 0.25 mg/ml; 0.5 mg/ml; and 1 mg/ml. **B**: Comparison of decreases in cell activity in the presence of ranibizumab after malignant melanoma cells were incubated in the cell system for about 72 h. * $p < 0.05$ compared to untreated cells. **C** and **D** show the dynamic response of ARPE-19 with different concentrations of ranibizumab, as follows: untreated cells (control); 0.1 mg/ml; 0.25 mg/ml; 0.5 mg/ml; and 1 mg/ml. **D**: Comparison of decreases in cell activity in the presence of ranibizumab after ARPE-19 cells were incubated in the cell system for about 72 h. * $p < 0.05$ compared to untreated cells. Data represents three independent experiment and all data points plotted as mean values \pm SD (* $p < 0.05$).

Uveal melanoma (UM) is an intraocular malignant tumor occurring mainly in Caucasian adults that usually originates from melanocytes of the choroid, iris, and ciliary body [34,35]. UM has an incidence of about 2–8 per million per year in Caucasians [36]. Immunohistochemistry has been the primary tool to distinguish melanomas from other tumors; it is also an adjunct tool to distinguish benign and malignant melanocytic tumors. Useful markers for melanoma include S-100 protein, which is highly sensitive, as well as HMB-45, Melan-A, tyrosinase, and microphthalmia-associated transcription factor (MITF), which are generally more specific [37]. In our study, the results of immunocytochemical staining of malignant melanoma cells and the primary tissue were basically similar; they both showed diffuse staining

of S-100 protein and HMB-45, while Melan-A was weakly positive.

The UM cells we cultured were abundant in pigmentation, but lacked pigment after several passages. It has been reported that the production of melanin pigment of human melanoma cells is dependent on tyrosine levels in medium [38]. The results from a nonspecific melanoma experimental model (B16 melanoma) suggested that primary tumors contain cells with variable growth characteristics and metastatic potential [39]. One study [40] focused on the isolation of seven human melanoma cell lines. In the cases derived from pigmented biopsy samples, cellular pigmentation increased as the cells became confluent; this observation was most striking in the multilayered clumps of cells that formed. This

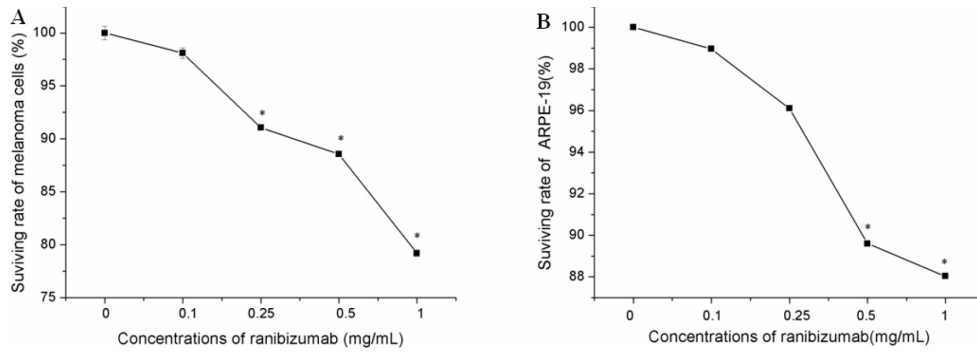


Figure 6. MTT assay for effects of ranibizumab on uveal melanoma cells and ARPE-19 cells. **A:** The dynamic response of malignant melanoma cells with different concentrations of ranibizumab: untreated cells (control); 0.1 mg/ml; 0.25mg/ml; 0.5mg/ml and 1mg/ml. **B:** The dynamic response of ARPE-19 with different concentrations of ranibizumab: untreated cells (control); 0.1 mg/ml; 0.25 mg/ml; 0.5 mg/ml and 1 mg/ml. Date represents four independent experiment and all data points plotted as mean values±SD (*p<0.05).

increase in melanin synthesis with increased cell density was accompanied by a parallel increase in tyrosinase synthesis. Cells grown in RPMI 1640 showed less pigmentation than those cultured in DME. As previously reported [41], the density-dependent increase in the rate of tyrosinase synthesis by UCT-Mel 2 could be inhibited by 10^{-6} M retinoic acid. Permanent cell lines (UCT-Mel 1 through 7) were established from biopsies of metastatic tissue taken from seven patients with malignant melanoma. University of Cape Town melanoma cell line 2 is the full name of UCT-Mel 2. Although

derived from tissue that was pigmented in vivo, UCT-Mel 4 cells could lose the pigment in vitro.

It has long been accepted that angiogenesis plays an important role in tumor growth, invasion, and eventually metastasis. VEGF was shown to be secreted by tumors and to stimulate angiogenesis [42]. In this study, we cultured the tumor specimen obtained from our clinic in vitro, and investigated whether ranibizumab played an inhibitory role in the growth of malignant melanoma. Using ELISA, we examined the VEGF expression levels in malignant melanoma cells and ARPE-19 affected by ranibizumab. The results showed that

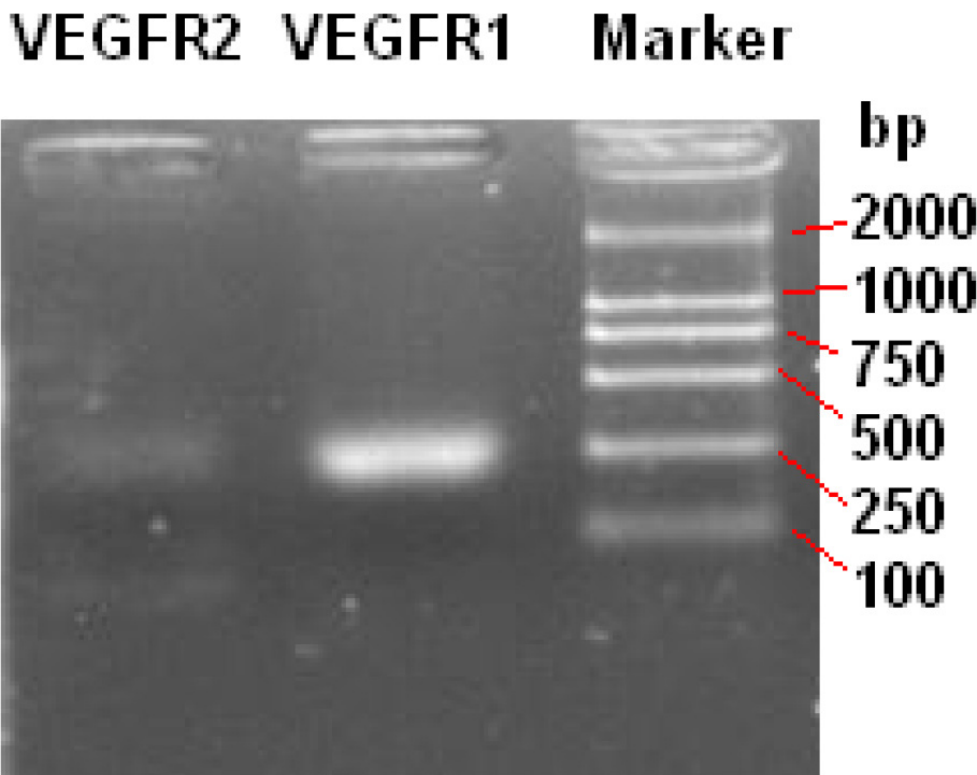


Figure 7. VEGF Receptor expression in human malignant melanoma of ciliary body. Total RNA from malignant melanoma of ciliary body was extracted from formalin-fixed, paraffin-embedded tissue and the expression of VEGFR1 and VEGFR2 was examined by RT-PCR.

the levels of VEGF secreted by malignant melanoma cells were much greater than those of ARPE-19, and the levels of VEGF of malignant melanoma cells declined markedly via the action of ranibizumab. On the other hand, there was no evident decrease of VEGF in the presence of ranibizumab for ARPE-19. When VEGF was added to the malignant melanoma cells, the viability of these cells increased greatly, and this increased kinetically following the culture time. However, there was no evident effect of VEGF on the cell proliferation of ARPE-19. Further research showed that the growth of malignant melanoma cells was obviously inhibited when ranibizumab intervened.

The signaling responses at the molecular level in UM need further investigation. It has been reported that the function of VEGFR family proteins is largely restricted to angiogenesis and regulation of vasculogenesis [43]. In this study, the expressions of VEGFR1 and VEGFR2 were examined by PCR.

Our findings indicate that malignant melanoma cells can express more VEGF, and the growth of tumor cells is VEGF dependent. In cell culture, the proliferation of malignant melanoma of the ciliary body can be restrained effectively by anti-VEGF agents. The possible mechanism of the inhibitory effect may be antagonizing VEGF through VEGFR1. In contrast, low-dose exposure of ranibizumab had a slight effect on the growth of ARPE-19. Only high-dose ranibizumab has an inhibitory effect on ARPE-19 cells.

In summary, our study suggests that ranibizumab can selectively inhibit malignant melanoma cell proliferation by decreasing the levels of VEGF. The possible mechanism of the inhibitory effect may be antagonizing VEGFR1. Moreover, our observations demonstrate that although ranibizumab can greatly inhibit ARPE-19 proliferation in vitro at higher concentrations, it has little effect on ARPE-19 at lower concentrations. As this is an in vitro study, which may not simulate the complicated human internal environment perfectly, further in vivo investigations are necessary for exploration of this mechanism.

ACKNOWLEDGMENTS

We gratefully acknowledge support from the Natural Science Foundation of Shandong Province (Grant Y2006C101). Yang Li served as experimental advisor.

REFERENCES

- Toi M, Bando H, Weich HA. Vascular endothelial growth factor and its relationships with endogenous inhibitors in a breast cancer microenvironment manipulated by hormonal therapy: a hypothetical consideration. *Biomed Pharmacother* 2005; 59:suppl2S344-7. [PMID: 16507406].
- Eming SA, Krieg T. Molecular mechanisms of VEGF-A action during tissue repair. *J Investig Dermatol Symp Proc* 2006; 11:79-86. [PMID: 17069014].
- Kiselyov A, Balakin KV, Tkachenko SE. VEGF/VEGFR signalling as a target for inhibiting angiogenesis. *Expert Opin Investig Drugs* 2007; 16:83-107. [PMID: 17155856].
- Laitinen M, Ristimäki A, Honkasalo M, Narko K, Paavonen K, Ritvos O. Differential hormonal regulation of vascular endothelial growth factors VEGF, VEGF-B, and VEGF-C messenger ribonucleic acid levels in cultured human granulosa-luteal cells. *Endocrinology* 1997; 138:4748-56. [PMID: 9348202].
- Lohela M, Saaristo A, Veikkola T, Alitalo K. Lymphangiogenic growth factors, receptors and therapies. *Thromb Haemost* 2003; 90:167-84. [PMID: 12888864].
- Wissmann C, Detmar M. Pathways targeting tumor lymphangiogenesis. *Clin Cancer Res* 2006; 12:6865-8. [PMID: 17145802].
- Shibuya M, Ito N, Claesson-Welsh L. Structure and function of vascular endothelial growth factor receptor-1 and -2. *Curr Top Microbiol Immunol* 1999; 237:59-83. [PMID: 9893346].
- Emerson MV, Lauer AK. Current and emerging therapies for the treatment of age-related macular degeneration. *Clin Ophthalmol* 2008; 2:377-88. [PMID: 19668729].
- Karagiannis DA, Ladas LD, Parikakis E, Georgalas I, Kotsolis A, Amariotakis G, Soumplis V, Mitropoulos P. Changing from bevacizumab to ranibizumab in age-related macular degeneration. Is it safe? *Clin Interv Aging* 2009; 4:457-61. [PMID: 20054410].
- Mitchell P, Bandello F, Schmidt-Erfurth U, Lang GE, Massin P, Schlingensiefel RO, Sutter F, Simader C, Burian G, Gerstner O, Weichselberger A. RESTORE study group. The RESTORE study: ranibizumab monotherapy or combined with laser versus laser monotherapy for diabetic macular edema. *Ophthalmology* 2011; 118:615-25. [PMID: 21459215].
- Hurwitz H, Fehrenbacher L, Novotny W, Cartwright T, Hainsworth J, Heim W, Berlin J, Baron A, Griffing S, Holmgren E, Ferrara N, Fyfe G, Rogers B, Ross R, Kabbinavar F. Bevacizumab plus irinotecan, fluorouracil, and leucovorin for metastatic colorectal cancer. *N Engl J Med* 2004; 350:2335-42. [PMID: 15175435].
- Finger PT. Radiation retinopathy is treatable with anti-vascular endothelial growth factor bevacizumab (Avastin) *Int J Radiat Oncol Biol Phys* 2008; 70:974-7. [PMID: 18313522].
- Ziemssen F, Voelker M, Altpeter E, Bartz-Schmidt KU, Gelissen F. Intravitreal bevacizumab treatment of radiation maculopathy due to brachytherapy in choroidal melanoma. *Acta Ophthalmol Scand* 2007; 85:579-80. [PMID: 17324216].
- Roland CL, Dineen SP, Lynn KD, Sullivan LA, Dellinger MT, Sadegh L, Sullivan JP, Shames DS, Brekken RA. Inhibition of vascular endothelial growth factor reduces angiogenesis and modulates immune cell infiltration of orthotopic breast

- cancer xenografts. *Mol Cancer Ther* 2009; 8:1761-71. [PMID: 19567820].
15. Roland CL, Lynn KD, Toombs JE, Dineen SP, Udugamasooriya DG, RA. Cytokine levels correlate with immune cell infiltration after anti-VEGF therapy in preclinical mouse models of breast cancer. *PLoS ONE* 2009; 4:[PMID: 19888452].
 16. Giantonio BJ, Catalano PJ, Meropol NJ, O'Dwyer PJ, Mitchell EP, Alberts SR, Schwartz MA. Bevacizumab in combination with oxaliplatin, fluorouracil, and leucovorin (FOLFOX4) for previously treated metastatic colorectal cancer: results from the Eastern Cooperative Oncology Group Study E3200. *J Clin Oncol* 2007; 25:1539-44. [PMID: 17442997].
 17. AVAIL. Reck M, von Pawel J, Zatloukal P, Ramlau R, Gorbounova V, Hirsh V, Leighl N, Mezger J, Archer V, Moore N, Manegold C. Phase III trial of cisplatin plus gemcitabine with either placebo or bevacizumab as first-line therapy for nonsquamous non-small-cell lung cancer. *J Clin Oncol* 2009; 27:1227-34. [PMID: 19188680].
 18. Sandler A, Gray R, Perry MC, Brahmer J, Schiller JH, Dowlati A, Lilenbaum R, Johnson DH. Paclitaxel-carboplatin alone or with bevacizumab for non-small-cell lung cancer. *N Engl J Med* 2006; 355:2542-50. [PMID: 17167137].
 19. Xing JZ, Zhu L, Jackson JA, Gabos S, Sun XJ, Wang XB, Xu X. Dynamic monitoring of cytotoxicity on microelectronic sensors. *Chem Res Toxicol* 2005; 18:154-61. [PMID: 15720119].
 20. Xing JZ, Zhu LJ, Gabos S, Xie L. Microelectronic cell sensor assay for detection of cytotoxicity and prediction of acute toxicity. *Toxicol In Vitro* 2006; 20:995-1004. [PMID: 16481145].
 21. Zhu J, Wang XB, Xu X, Abassi YA. *Immunol J Methods* 2006; 309:25-33. .
 22. Guo D, Bi H, Wang D, Wu Q. Zinc oxide nanoparticles decrease the expression and activity of plasma membrane calcium ATPase, disrupt the intracellular calcium homeostasis in rat retinal ganglion cells. *Int J Biochem Cell Biol* 2013; 45:1849-59. [PMID: 23764618].
 23. Rupp GM, Locker J. Purification and analysis of RNA from paraffin-embedded tissues. *Biotechniques* 1988; 6:56-60. [PMID: 2483655].
 24. Hou JX, Li SY, Liu WJ, Yang HY. Application of Giemsa staining in melanocytic lesions with immunohistochemical counter staining. *Clin Exp Pathol* 1996; 12:178-.
 25. Ferrara N, Gerber HP, LeCouter J. The biology of VEGF and its receptors. *Nat Med* 2003; 9:669-76. [PMID: 12778165].
 26. Murakami M, Zheng Y, Hirashima M, Suda T, Morita Y, Ooehara J, Ema H, Fong GH, Shibuya M. VEGFR1 tyrosine kinase signaling promotes lymphangiogenesis as well as angiogenesis indirectly via macrophage recruitment. *Arterioscler Thromb Vasc Biol* 2008; 28:658-64. [PMID: 18174461].
 27. Tchaikovski V, Fellbrich G, Waltenberger J. The molecular basis of VEGFR-1 signal transduction path-ways in primary human monocytes. *Arterioscler Thromb Vasc Biol* 2008; 28:322-8. [PMID: 18079407].
 28. Carmeliet P, Moons L, Luttun A, Vincenti V, Compernelle V, DeMolM, Wu Y, Bono F, Devy L, Beck H, Scholz D, Acker T, DiPalma T, Dewerchin M, Noel A, Stalmans I, Barra, A, Blacher S, Vandendriessche T, Ponten A, Eriksson U, Plate KH, Foidart JM, Schaper W, Charnock-Jones DS, Hicklin DJ, Herbert JM, Collen D, Persico G. Synergism between vascular endothelial growth factor and placental growth factor contributes to angiogenesis and plasma extravasation in pathological conditions. *Nat Med* 2001; 7:575-83. [PMID: 11329059].
 29. Schwartz JD, Rowinsky EK, Youssoufian H, Pytowski B, Wu Y. Vascular endothelial growth factor receptor-1 in human cancer: Concise review and rationale for development of IMC-18F1 (Human antibody targeting vascular endothelial growth factor receptor-1). *Cancer* 2010; 116:1027-32. [PMID: 20127948].
 30. Byrne AM, Bouchier-Hayes DJ, Harmey JH. Angiogenic and cell survival functions of Vascular Endothelial Growth Factor (VEGF). *J Cell Mol Med* 2005; 9:777-94. [PMID: 16364190].
 31. Kabbinavar F, Hurwitz HI, Fehrenbacher L, Meropol NJ, Novotny WF, Liberman G, Griffing S, Bergsland E. Phase II, randomized trial comparing bevacizumab plus fluorouracil (FU)/leucovorin (LV) with FU/LV alone in patients with metastatic colorectal cancer. *J Clin Oncol* 2003; 21:60-5. [PMID: 12506171].
 32. Yang JC, Haworth L, Sherry RM, Hwu P, Schwartzentruber DJ, Topalian SL, Steinberg SM, Chen HX, Rosenberg SA. A randomized trial of bevacizumab, an antivascular endothelial growth factor antibody, for metastatic renal cancer. *N Engl J Med* 2003; 349:427-34. [PMID: 12890841].
 33. Chen Y, Wiesmann C, Fuh G, Li B, Christinger HW, McKay P, Vos AM, Lowman HB. Selection and analysis of an optimized anti-VEGF antibody: crystal structure of an affinity-matured Fab in complex with antigen. *J Mol Biol* 1999; 293:865-81. [PMID: 10543973].
 34. Singh AD, Topham A. Survival rates with uveal melanoma in the United States: 1973–1997. *Ophthalmology* 2003; 110:962-5. [PMID: 12750098].
 35. Horland PG, Clement T. Genomic Investigations of Posterior Uveal Melanoma. *Semin Ophthalmol* 2005; 20:231-8. [PMID: 16352494].
 36. Damato B. Does ocular treatment of uveal melanoma influence survival? *Br J Cancer* 2010; 103:285-90. [PMID: 20661247].
 37. Ohsie SJ, Sarantopoulos GP, Cochran AJ, Binder SW. Immunohistochemical characteristics of melanoma. *J Cutan Pathol* 2008; 35:433-44. [PMID: 18399807].
 38. Slominski A, Zbytek B, Slominski R. Inhibitors of melanogenesis increase toxicity of cyclophosphamide and lymphocytes against melanoma cells. *Int J Cancer* 2009; 124:1470-7. [PMID: 19085934].
 39. Aubert C, Voulot C, Rouge F, Pirisi V, Galinda JR. New variants of B16 mouse melanoma: differentiation and metastatic

- properties. *Pigment Cell Res* 1989; 2:17-25. [PMID: 2717526].
40. Hoal-Van Helden EG, Wilson EL, Dowdle EB. Characterization of seven human melanoma cell lines: Melanogenesis and secretion of plasminogen activators. *Br J Cancer* 1986; 54:287-95. [PMID: 3091056].
41. Azar HA, Hansen CT, Costa J. II-nu/nu mice combined immunodeficiency: a new model for human tumour heterotransplantation. *J Natl Cancer Inst* 1980; 65:421- [PMID: 6967528].
42. Dvorak HF, Brown LF, Detmar M, Dvorak AM. Vascular permeability factor/vascular endothelial growth factor, microvascular hyperpermeability, and angiogenesis. *Am J Pathol* 1995; 146:1029-39. [PMID: 7538264].
43. Olsson A-K, Dimberg A, Kreuger J, Claesson-Welsh L. VEGF receptor signaling-in control of vascular function. *Nat Rev Mol Cell Biol* 2006; 7:359-71. [PMID: 16633338].
44. Olsson A-K, Dimberg A, Kreuger J, Claesson-Welsh L. VEGF receptor signaling-in control of vascular function. *Nat Rev Mol Cell Biol* 2006; 7:359-71. [PMID: 16633338].

Articles are provided courtesy of Emory University and the Zhongshan Ophthalmic Center, Sun Yat-sen University, P.R. China. The print version of this article was created on 13 May 2014. This reflects all typographical corrections and errata to the article through that date. Details of any changes may be found in the online version of the article.